European Journal of Pharmaceutical Sciences 199 (2024) 106813

Contents lists available at ScienceDirect

European Journal of Pharmaceutical Sciences

journal homepage: www.elsevier.com/locate/ejps

Synthesis and estrogenic activity of BODIPY-labeled estradiol conjugates

Miroslav Peřina [a,1], Rita Börzsei [b,1], Henrietta Ágoston [c,1], Tamás Hlogyik [c], Miklós Poór [d,e], Réka Rigó [f], Csilla Özvegy-Laczka [f], Gyula Batta [g], Csaba Hetényi [b], Veronika Vojáčková [a], Radek Jorda [a,*], Erzsébet Mernyák [c,h,*]

[a] Department of Experimental Biology, Faculty of Science, Palacký University Olomouc, Šlechtitelů 27 78371 Olomouc, Czech Republic
[b] Department of Pharmacology and Pharmacotherapy, Medical School, University of Pécs, Szigeti út 12 H-7624 Pécs, Hungary
[c] Department of Inorganic, Organic and Analytical Chemistry, University of Szeged, Dóm tér 7–8 H-6720 Szeged, Hungary
[d] Department of Laboratory Medicine, Medical School, University of Pécs, Ifjúság útja 13, Pécs H-7624, Hungary
[e] Molecular Medicine Research Group, János Szentágothai Research Centre, University of Pécs, Ifjúság útja 20, Pécs H-7624, Hungary
[f] Drug resistance research group, Institute of Enzymology, Research Centre for Natural Sciences, Magyar tudósok körútja 2, H-1117 Budapest, Hungary
[g] Department of Organic Chemistry, University of Debrecen, Egyetem tér 1 H-4032 Debrecen, Hungary
[h] Department of Pharmacognosy, University of Szeged, Eötvös u. 6 H-6720 Szeged, Hungary

ARTICLE INFO

Keywords:
17β-estradiol
BODIPY
CuAAC
Estrogenic activity
Human estrogen receptor alpha

ABSTRACT

Novel BODIPY–estradiol conjugates have been synthesized by selecting position C-3-*O* for labeling. The conjugation strategy was based on Cu(I)-catalyzed azide–alkyne cycloaddition (CuAAC) or etherification. Estradiol derivatives used as azide partners bearing an ω-azidoalkyl function through C_4–C_8-long linkers have been prepared. CuAAC reactions of estradiol azides with BODIPY alkyne furnished fluorescent 3-*O*-labeled conjugates bearing the triazole ring as a coupling moiety. Williamson etherifications of 3-*O*-(ω-bromoalkyl)-17β-estradiol derivatives with BODIPY-OH resulted in labeled conjugates connected with an ether moiety. Interactions of the conjugates with estrogen receptor (ER) were investigated using molecular docking calculations in comparison with estradiol. The conjugates occupied both the classical and alternative binding sites on human ERα, with slightly lower binding affinity to references estradiol and diethystilbestrol. All compounds have displayed reasonable estrogenic activity. They increased the proliferation of ER-positive breast cancer cell line MCF7 contrary to ER-negative SKBR-3 cell line. The most potent compound **13a** induced the transcriptional activity of ER in dose-dependent manner in dual luciferase recombinant reporter model and increased progesterone receptor's expression, proving the retained estrogenic activity. The fluorescence of candidate compound **13a** co-localised with the ERα. The newly synthesized labeled compounds might serve as good starting point for further development of fluorescent probes for modern biological applications. In addition to studying steroid uptake and transport in cells, e.g. in the processes of biodegradation of estrogen-hormones micropollutants, they could also be utilized in examination of estrogen-binding proteins.

1. Introduction

17β-Estradiol (E2) is the most potent female steroid hormone. It controls the development and maintenance of female sex characteristics. However, its overproduction stimulates the proliferation of hormone-sensitive cells, leading to hormone-dependent diseases (Miller and Auchus, 2011; Gupta et al., 2013). One of the therapeutic approaches in estrogen-dependent cancers is based on inhibition of the biosynthesis of E2. Estrogens are mainly synthesized in ovaries and the placenta *via* enzymatic reactions catalyzed by steroid sulfatase, aromatase, and 17β-hydroxysteroid dehydrogenase 1 (Hong and Chen, 2011; Marchais-Oberwinkler et al., 2011). Nevertheless, *de novo* synthesis of estrogens occurs in various non-reproductive tissues including the brain (Azcoitia et al., 2011). Certain enzymes responsible for the synthesis of E2 have been identified in neurons and glial cells, that is, E2 can be regarded not only as a female hormone but as a 'neurosteroid' too (Pelletier, 2010). Consequently, estrogens can modulate essential brain functions. Numerous literature reports describe important

* Corresponding authors.
E-mail addresses: radek.jorda@upol.cz (R. Jorda), bobe@chem.u-szeged.hu, mernyak.erzsebet@szte.hu (E. Mernyák).
[1] These authors contributed equally to this work.

https://doi.org/10.1016/j.ejps.2024.106813
Received 24 March 2024; Received in revised form 17 May 2024; Accepted 23 May 2024
Available online 24 May 2024

neuroprotective roles of E2 in neurodegenerative diseases (Cespedes Rubio et al., 2018). Concerning the diverse biological importance of the main estrogen E2, it would be of particular interest to establish the mechanism of its biological actions. In order to acquire information about its interactions with certain proteins, including receptors or enzymes, their appropriate labeling is essential. Several biochemical assays exist based on radioisotope labeling; however, there is an increasing demand for benign and greener bioanalytical methods. Fluorescent labeling could serve as a more favorable alternative. Beside the advantages of this green approach, several limits might arise. The fluorescent dyes are usually relatively large molecules containing more rings and diverse functional groups. Coupling of such compounds with biomolecules might greatly influence the original biological behavior. The position of labeling, the spacing between the labeled compound and the dye, and the coupling moiety might all determine biological applicability. Concerning the fluorescent dye, there are several points that should be taken into account. Key characteristics, are the feasibility of its synthesis, chemical and metabolic stability, and good fluorescent properties. 4,4-Difluoro-4-bora-3a,4a-diaza-*s*-indacenes (BODIPYs) meet all these criteria (Ulrich et al., 2008; Loudet and Burgess, 2007; Karolin et al., 1994; Haugland, 1996). Therefore, BODIPY-based labeling of different types of biomolecules, including nucleic acids, saccharides, and steroids, is emerging. Only a few BODIPY-labeled estrogens are known, which are mainly conjugated at the C-3, C-7 or C-17 positions prepared *via* different couplings, including Sonogashira or Cu (I)-catalyzed azide–alkyne click reaction (CuAAC) (Osati et al., 2016; Osati et al., 2017; Liang and Astruc, 2011; Langhals and Obermeier, 2008; Felion et al., 2022). Felion et al. (Felion et al., 2022) described the synthesis of BODIPY-labeled estrogens *via* click-strategy starting from the C-3-*O* propargylated derivatives. This procedure allowed the synthesis of conjugates bearing only one-carbon–long linker between the steroid and the triazole ring. The BODIPY core and the triazole moiety were attached via a propyl linker. The authors highlighted the usage of newly synthesized labeled estradiol as a probe for studying biodegradation using an estrogen-catabolizing bacterium. We have published recently the synthesis of BODIPY–estrone conjugates **5**–**7** labeled at positions C-2 or C-15 (Fig. 1) (Bacsa et al., 2018). Our coupling strategy involved CuAAC reactions of an estrone–azide or estrone–alkynes with the complementary BODIPY azide **3** or BODIPY alkyne **4**. Three new fluorescent estrone conjugates (**5**–**7**) were synthesized (Fig. 1). We paid particular attention to leave the main oxygen functionalities (at C-3 and C-17) of estrone (E1, **1a**) intact. The measured fluorescence properties of the compounds (**5**–**7**) suggest that they might be applicable for their observation in living cells.

Literature data suggest that even though the 3- and 17-oxygen functionalities of estrogens are regarded as necessary moieties for receptor binding, fluorescent labeling at the 3-OH group might result in compounds with retained biological properties. Estradiol glow (**8**, Fig. 2) is a fluorescent conjugate of E2 labeled at position C-3-*O* with a low-molecular-weight orange/red fluorophore (Jirikowski and Reimar). The latter moiety and the steroid are connected by an eight-carbon-long linker. Even though the steroid is labeled at its phenolic OH function, its estrogenic action is similar to that of E2. Considering that a labeled estrogen could allow determination of steroid uptake, transport, and binding to certain proteins on a single-cell level, the understanding of the mechanism of action of such compounds would be of particular interest.

In this study we focused on the synthesis of novel E2 conjugates labeled at C-3-*O* (Fig. 3). The labeling was planned with BODIPY derivatives as fluorescent moieties containing a terminal alkyne or a phenolic hydroxy function. These structural elements allow the coupling of the BODIPY to the steroid *via* CuAAC or etherification. We aimed to synthesize the conjugates *via* inserting C_4–C_8-long linkers between the steroid and the dye. The determination of the estrogenic activity of the conjugates was intended on MCF7 (ER-positive) and SKBR-3 (ER-negative) breast cancer cell lines. Docking and intermolecular binding energy

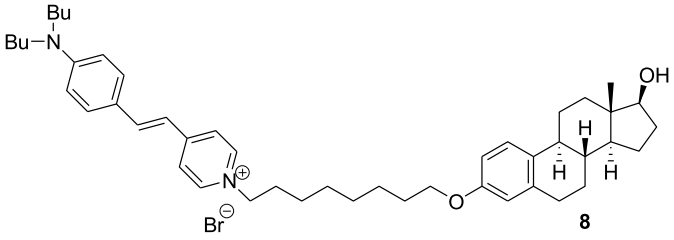

Fig. 2. Estradiol glow (**8**).

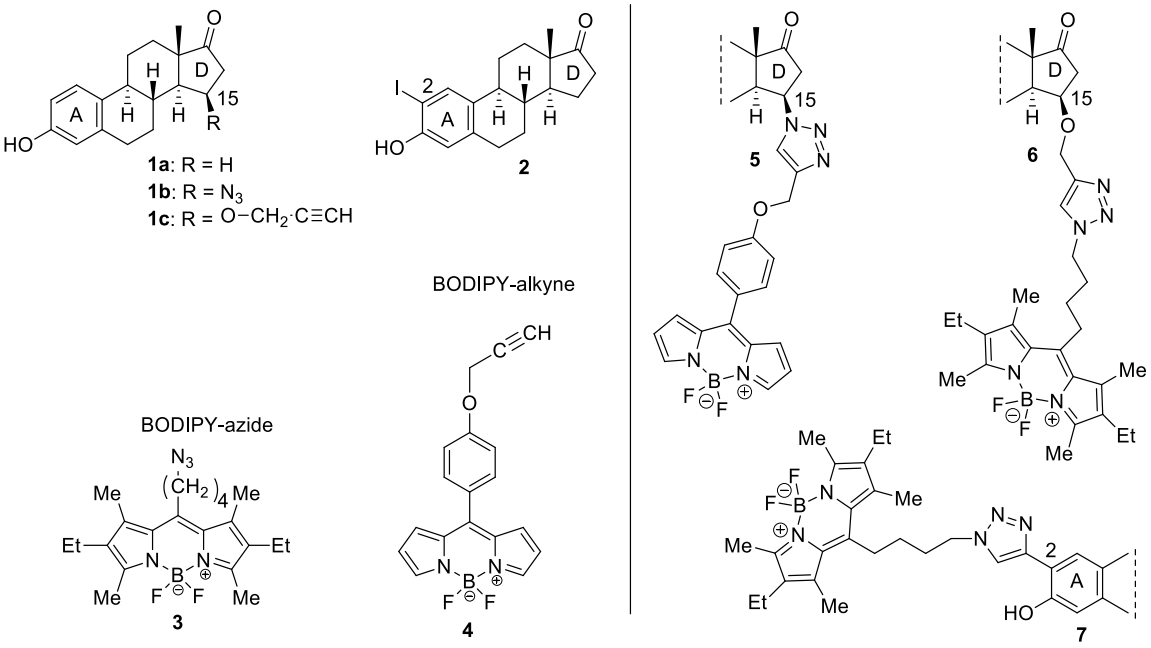

Fig. 1. BODIPY–estrone conjugates (**5**–**7**) synthesized recently and their fluorescent building blocks (**1**–**4**).

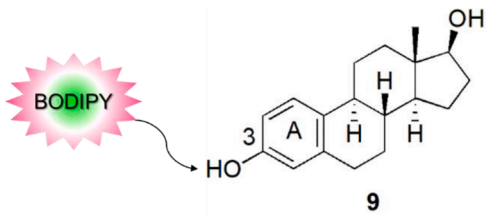

Fig. 3. Fluorescent labeling of 17β-estradiol E2 (**9**).

calculations were performed to investigate the binding mode and strength of the newly synthesized conjugates.

2. Results and discussion

2.1. Synthesis

First the syntheses of BODIPY derivatives bearing terminal alkyne or phenolic hydroxy function were performed. The synthesis of BODIPY alkyne **4** was carried out *via* our efficient methodology described earlier (Bacsa et al., 2018). The depropargylation reaction was achieved using $Pd(OAc)_2$ under microwave irradiation, leading to compound 4a in high yield (Scheme 1).

The steroidal starting compounds (**10a–c, 11a–c**) suitable for cycloadditions or etherifications were synthesized according to Scheme 2. The introduction of linkers onto E2 was achieved by alkylating the phenolic OH function with three different α,ω-dibromoalkanes, containing even-numbered carbon chains (**4, 6**, and **8**). We believe that the linker length might be one of the determining factors concerning the biological behavior of the fluorescent conjugate. Etherifications were achieved in high yields using K_2CO_3 as base and 18-crown-6 as additive. In the next reaction step, substitution of the ω-bromine with azide nucleophile using NaN_3 in DMSO solvent was performed. The resulting E2-azides (**11a–c**) served as key intermediates in the synthesis of E2-BODIPY conjugates 12a–c coupled *via* the formation of the triazole ring. CuAAC reactions of the steroidal azides (**11a–c**) and the BODIPY alkyne (**4**) were achieved *via* our highly efficient click methodology established earlier (Szabo et al., 2016; Kadar et al., 2011; Kadar et al., 2012; Mernyak et al., 2015; Szabó et al., 2016). Compounds **12a–c**, which differ in length of the freely rotating linker, might allow the investigation of the linker-dependent biological behavior of fluorescent estrogens. These BODIPY conjugates (**12a–c**) are expected to have high chemical and metabolic stability thanks to their building blocks and the triazole coupling moiety (Pedersen and Abell, 2011).

The synthesis of these new E2-BODIPY triazoles (**12a–c**) required three synthetic steps, including etherification, nucleophilic substitution, and the CuAAC reaction. In order to decrease the number of reaction steps, ω-bromo intermediates (**10a–c**) have directly been subjected to fluorescent labeling *via* etherification (Scheme 2). Couplings of ω-bromo

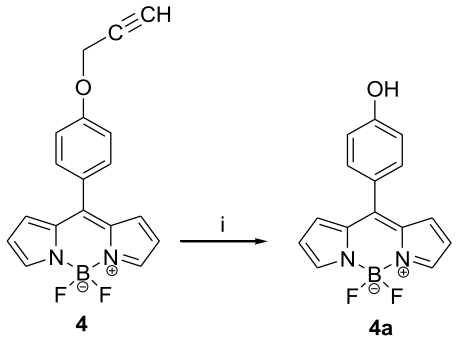

Scheme 1. Reagents and conditions: (i) $Pd(OAc)_2$ (0.05 equiv.), 150 °C, MW, toluene, 30 min.

intermediates (**10a–c**) with 4′-hydroxy-BODIPY (4a) resulted in the desired conjugates (**13a–c**) in high yields.

The two types of BODIPY derivatives **4** and **4a** as well as the three pairs of estradiol derivatives (**10a–c** and **11a–c**) allowed the efficient syntheses of BODIPY-estradiol conjugates differing in the coupling moiety and the distance between the steroid and the dye.

The structures of the newly synthesized fluorescent E2 derivatives (**12a–c** and **13a–c**) and the intermediates (**10a–c** and **11a–c**) were deduced from ^{1}H and ^{13}C NMR spectra.

2.2. Molecular docking

Docking calculations were performed to investigate and compare the binding mode of the newly synthesized E2-BODIPY conjugates to the natural 17β-Estradiol (E2) and diethystilbestrol (DES) on the human estrogen receptor alpha (hERα). The validity of the docking method is represented by the low RMSD values calculated for the docked and experimental conformations of the E2 and DES, specifically 2.1 Å (Bálint et al., 2017) and 0.7 Å (present study), respectively. It is known from previous studies that there are two binding sites of E2 on hERα including a classical (CBS) and an alternative (ABS) binding site separated by a salt bridge between E353 and R394 from each other (Bálint et al., 2017; Norman et al., 2004; van Hoorn, 2002). ABS was suggested to mediate the non-classical effects of E2 (Bálint et al., 2017; van Hoorn, 2002), while E2 binding into the CBS is responsible for genomic effects (Bálint et al., 2017). Docking calculations were performed for both an apo and a holo conformation of hERα. The fluorescent E2-BODIPY conjugates docked into both the ABS and CBS *via* their steroid fragment (Fig. 4A) with conformation and interaction patterns similar to those of E2. Interestingly, DES docked only in CBS and does not occupy ABS.

The global view of compound **12a** binding shows that ABS is more exposed to the bulk than CBS and it is covered only with a highly flexible loop (Fig. 4A), which might make it more accessible for larger ligands. The binding conformation and interaction pattern of the natural E2 and the steroid fragment of the BODIPY derivatives show an excellent overlap in both ABS and CBS (Fig. 4B), as reflected by the list of target residues interacting with the ligands within a 3.5 Å distance in Supporting Table 1, 2. The calculated per-atom binding affinity in terms of efficiency indices (EI=-ΔG_b/NHA, where ΔG_b is the estimated binding free energy of a ligand, NHA is the number of heavy atoms in a ligand, Supporting Information Table 1) also shows a better binding to hERα in the cases of E2 and DES if compared with the BODIPY conjugates 12 and 13.

Figs. 4C and 4D show the close-up view of compounds with the best EIs, such as **12a** (0.26) and **13a** (0.24) in the CBS and ABS, respectively. Compound **12a** in CBS creates interaction with H524 *via* its C17 hydroxy group similar to that of natural E2 (Bálint et al., 2017; Kousteni et al., 2002; Anstead et al., 1997), which is essential for ligand binding and estrogenic activity. The C-3-*O*—C moiety of all BODIPY conjugates interact with E353 and R394 of hERα suggested to adjust the steroid scaffold into the active conformation similar to the case of E2 (Brzozowski et al., 1997). The nonpolar steroid moiety fits into the hydrophobic pocket created by several leucines, glycine, and phenylalanine (Supporting Table 1). The BODIPY moiety hangs out from the plane of the receptor to the bulk [**12b, 13c**] or turns back [**12a, 12c, 13b**]. In the latter case, the difluoro-bora group of BODIPY derivatives interacts with residues of Helix 6 (W383-R394) and the subsequent loop of hERα such as W393, E397, and H398 (Fig. 4C).

In ABS the C17 hydroxy group of compound **13a** is connected with the backbone atoms of L387 *via* hydrogen bonding. The C3 phenolic OH of E2 creates H-bond with W393 of hERα. This interaction also develops in the case of the C-3-*O*-conjugated derivatives through the non-bonding electron pair of oxygen (Fig. 4D).

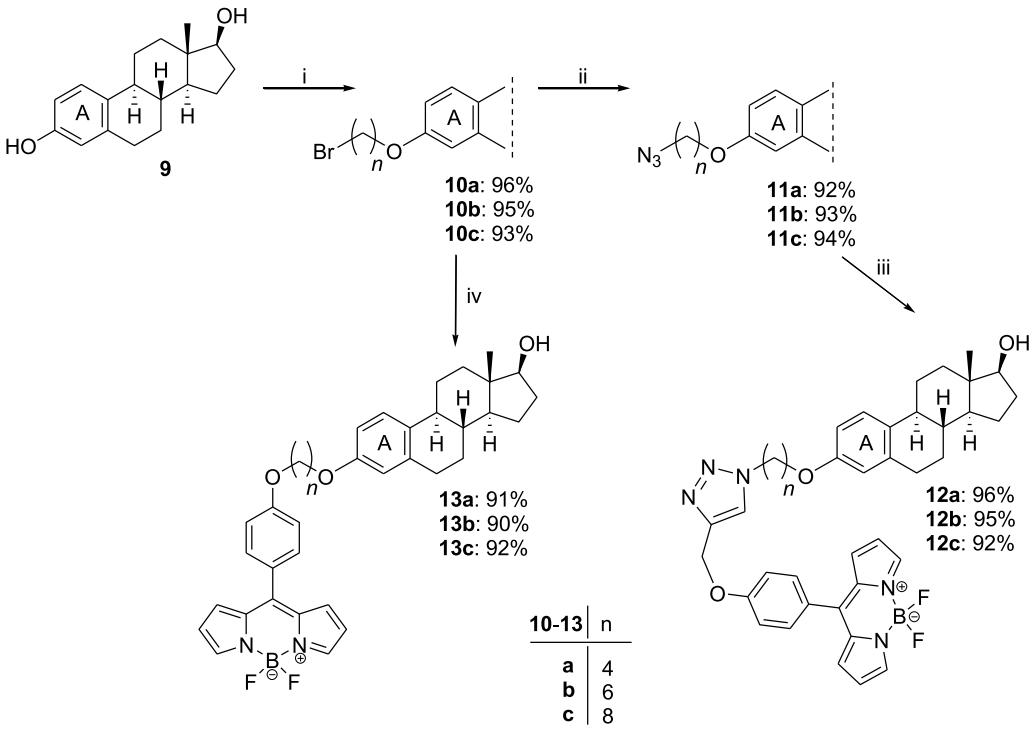

Scheme 2. Reagents and conditions: (i) α,ω-dibromoalkane (8 equiv.), K_2CO_3 (4 equiv.), 18-crown-6 (0.08 equiv.), 110 °C, toluene, N_2 atmosphere, 24 h; (ii) NaN_3 (2 equiv.) DMSO, rt (room temperature), 2 h; (iii) BODIPY alkyne 4 (1 equiv.), CuI (0.05 equiv.), Ph_3P (0.1 equiv.), DIPEA (3 equiv.), toluene, reflux, 2 h; (iv) BODIPY 4a (0.5 equiv.), K_2CO_3 (2 equiv.), 18-crown-6 (0.04 equiv.), 110 °C, toluene, N_2 atmosphere, 24 h.

2.3. Fluorescence spectra of E2 derivatives

To examine the fluorescence signals of the newly synthesized compounds, their excitation and emission spectra were recorded in dimethyl formamide (DMF) and in sodium phosphate buffer (0.05 M, pH 7.4). In DMF, the reference compound **4** and E2 derivatives exerted strong fluorescence, showing their excitation and emission wavelength maxima at 498 nm and at 515 nm, respectively (Fig. 5A and B): **13a** has the highest, while **12c** has the lowest emission signals among the compounds tested. Furthermore, in phosphate buffer, E2 derivatives showed their excitation maxima approximately at 510 nm and their emission wavelength maxima were observed around 560 nm, where **13a** and **12c** exerted the largest and the lowest emission signals, respectively (Fig. 5C and D).

2.4. Evaluation of biological activity

To test the estrogenic activity (agonist activity towards the ER), we performed the analysis of MCF7 (ER-positive) and SKBR-3 (ER-negative) cell proliferation after 72-hour treatment with novel E2-conjugates. We observed a significant increase in viability of MCF7 cells contrary to SKBR-3 cells (Table 1, Supplementary Figure S1). All conjugates displayed high estrogenic activity, with a sharp dose-dependent increase in the viability of MCF7 from the control level to about 175–230 % of untreated control. The maximal effect was observed at 10^{-6} M concentration, with compounds **12c** and **13a** being the most potent ones (Table 1). The increase in viability was consistent with the effect of free E2, which reached maximum between 10^{-11} M and 10^{-10} M concentrations (Supplementary Figure S1). These preliminary results indicated that conjugates retain estrogenic activity.

Next, we have analyzed another estrogenic effect of our novel compounds. It is well known, that progesterone receptor (PR) is a downstream target of ER and induction of ER activity drives the expression of PR (Marino et al., 2006; Fazzari et al., 2001).

Therefore, at first, we performed the 24-h treatment of MCF7 cells with free E2 and conjugates from series **12** and **13** in charcoal-stripped serum (CSS)-supplemented medium without phenol red. All compounds were able to induce strong increase in expression of PRα/β, while they decreased the protein level of ER slightly, similar to the effect of E2 (Fig. 6A). To choose the compound with the strongest estrogenic activity, we repeated the experiment with the treatment for 4 h. Only compound **13a** was able to increase the expression of PRα/β, similar to E2 after 4 h (Fig. 6B). Based on the results obtained from the proliferation assay of MCF7 cells (Supplementary Figure S1) and the above-mentioned effect on ERα signaling, compound **13a** with the highest estrogenic activity was considered to be the lead compound.

We proved that the lead compound **13a** induced the protein expression of PRα/β readily from 125 nM concentration, along with the decrease in ERα protein level, both in dose-dependent manner (Fig. 7A). Similarly, we observed a clear dose-dependent activation of the ER-transcriptional activity in the luciferase reporter assay in transfected SKBR-3 cells. The agonist activity of compound **13a** peaked in 2 μM concentration, while it reached similar potency to natural agonist E2 (used in 8 nM concentration) in range of 80 nM – 400 nM (Fig. 7B), which is in agreement with the downstream signaling analyzed by western blot (Fig. 6, 7A).

To confirm direct interaction of **13a** with recombinant ERα we performed competitive binding assay with the radioligand [3*H*]estradiol. The Ki value of **13a** was determined to be 190 nM (Supplementary figure S2).

Next, we evaluated the activity of conjugates to penetrate the cells by measuring their fluorescence in the cells. It was obvious that E2-BODIPY conjugates potently penetrate the MCF7 cells already after a 1-h treatment in 10 μM concentration and induce cellular fluorescence. The most potent compounds, which yielded the most intensive fluorescence, were **13a** and **13b**. On the other hand, none of compounds was able to induce reasonable fluorescence in 1 μM (Supplementary Figure S3). Next, we cultivated the MCF7 cells with fluorescent conjugates for 4 h followed by staining the nuclei. After a 4-h treatment, the most intensive green cellular fluorescence was observed after treatment with **13a**. On the

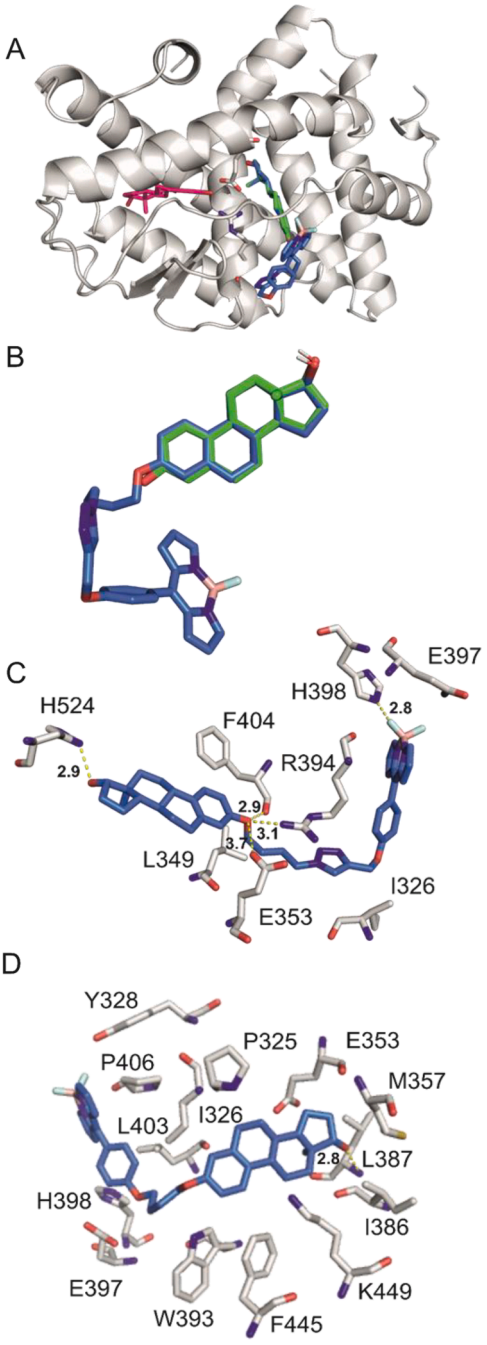

Fig. 4. **(A)** Binding pose of the natural E2 in the classical (CBS, magenta, sticks) and the alternative (ABS, green, sticks) binding sites of hERα. The binding sites are separated by a salt bridge between E353 and R394 that also interacts with the C3 phenolic hydroxy group of E2 in CBS. The binding pose of compound **12a** (blue, sticks) in ABS is also shown. **(B)** E2 perfectly overlaps with the steroid fragment of compound **12a** (blue, sticks) in ABS. **(C-D)** The close-up view of compounds **12a** and **13a** in the CBS and ABS, respectively (hERα residues are in grey sticks). H-bonds are shown as yellow dashed lines.

basis of nuclei staining, it seemed that the green fluorescence was localized mainly in cytosol, while most of the nuclei seemed to be unstained (Supplementary Figure S3).

We further investigated the ability of compounds to enter the nuclei by measuring their fluorescence in isolated cell nuclei using flow cytometry. We revealed that there is a clear difference between the autofluorescence of DNA in nuclei and the fluorescence of **13a,** which means that reasonable fraction of **13a** penetrated the nuclei. The intensity of green fluorescence of nuclei was dose dependent. Nearly 100 % of nuclei were stained upon treatment with 10 μM **13a** (Supplementary Figure S4).

In order to further evaluate the localization of E2-BODIPY conjugates, we performed the confocal microscopy of MCF7 cell upon the treatment with 10 μM **13a** for 4 h. We obtained similar results, observing a sharp green fluorescence of **13a** mainly in the cytosol (Fig. 8A). The image analysis of the co-localisation of **13a**-green and nuclei-red fluorescence signal revealed the slight overlap of signals equal to 16.88 ± 2.13 % (Pearsons' coefficient =0.238 ± 0.042) (Supplementary Table S3).

Based on the previously obtained results (induction of signaling, interaction with recombinant ERα and its transactivation) upon **13a** treatments, we were also interested in the co-localisation of **13a** and ERα in cells. We confirmed a clear overlap of **13a**-green fluorescence with signal of immuno-stained ERα (Fig. 8B), equal to 83.23 ± 2.80 (Pearsons' coefficient = 0.664 ± 0.049) (Supplementary Table S3).

3. Materials and methods

3.1. Chemistry

General

Melting points (m.p.) were determined with a Kofler hot-stage apparatus and are uncorrected. Elemental analyses were performed with a Perkin-Elmer CHN analyzer model 2400. Thin-layer chromatography: silica gel 60 F_{254}; layer thickness 0.2 mm (Merck); eluent: a: 5 % EtOAc/95 % CH_2Cl_2, b: 30 % EtOAc/70 % hexane, c: 20 % EtOAc/80 % CH_2Cl_2, d: 15 % EtOAc/85 % CH_2Cl_2. If otherwise not stated, detection with I_2 or UV (365 nm) after spraying with 5 % phosphomolybdic acid in 50 % aqueous phosphoric acid and heating at 100–120 °C for 10 min. Flash chromatography: silica gel 60, 40–63 μm (Merck). Reactions under microwave irradiation were carried out with a CEM Corporation focused microwave system, Model Discover SP. The ^{1}H NMR spectra were recorded in DMSO-d_6 or $CDCl_3$ solution with a Bruker DRX-500 instrument at 500 MHz, with Me_4Si as an internal standard. The ^{13}C NMR spectra were recorded with the same instrument at 125 MHz under the same conditions. Absorption (at fixed 620 nm emission wavelengths) and emission (at fixed 400 nm excitation wavelength) spectra were measured using an Enspire plate reader (Perkin Elmer, Waltham, MA, USA).

3.1.1. Synthesis of compound *4a*

Compound **4** (322 mg, 1.0 mmol), $Pd(OAc)_2$ (11.2 mg, 0.05 mmol) and toluene (5 mL) were added into a 35 ml Pyrex pressure vessel (CEM, Part #: 908,035) with silicone cap (CEM, Part #: 909,210). The mixture was irradiated in a CEM microwave reactor at 150 °C for 30 min under stirring. The solvent was evaporated in vacuo and the residue was purified by flash chromatography. with EtOAc/CH_2Cl_2 = 2/98 as an eluent. Compound **4a** was obtained as an orange solid (260 mg, 92 %). BODIPY derivative **4a** was identical with compound described in the literature (Farfan-Paredes et al., 2020). M.p.: 149.5–150.9 °C. Anal calcd. for $C_{15}H_{11}BF_2N_2O$: C, 63.42; H, 3.90. Found: C, 66.49; H, 3.86.

3.1.2. Synthesis of the steroidal bromides *10a–c*

General procedure

272 mg (1.0 mmol) of 17β-estradiol, 553 mg (4.0 mmol) of anhydrous, pre-dried potassium carbonate, and 20 mg (0.076 mmol) of 18-crown-6 were dissolved in 26 mL of dry toluene, then 1.1, 2.0 or 2.2 g (8.0 mmol) of 1,4-dibrombutane, 1,6-dibromhexane or 1,8-dibromoctane was added to the solution. The reaction mixture was stirred at 110 °C for 24 h under N_2 atmosphere. It was worked up by adding 50 mL of water, 10 mL of ethyl acetate and stirred for about 10 min. The phases were separated and the aqueous phase was extracted with 30 mL of solvent. The combined organic phases were dried over sodium sulfate, and the solvent was removed under reduced pressure. The residue was

Table 1
Proliferation of MCF7 and SKBR-3 upon the 72 h treatment with conjugates and E2.

Viability of cells [a]								
	MCF7 1 μM	p-value	SKBR-3 1 μM	p-value	MCF7 0.1 μM	p-value	SKBR-3 0.1 μM	p-value
12a	189.6 ± 13.4	0.0110 (*)	106.6 ± 4.4	0.1732 (ns)	172.1 ± 23.1	0.0476 (*)	118.1 ± 1.6	0.0039 (**)
12b	197.1 ± 8.5	0.0038 (**)	117.0 ± 15.0	0.2518 (ns)	178.3 ± 2.6	0.0006 (***)	119.6 ± 2.9	0.0109 (*)
12c	224.1 ± 11.7	0.0044 (**)	116.5 ± 25.4	0.4551 (ns)	179.0 ± 1.2	0.0001 (***)	118.5 ± 13.1	0.1849 (ns)
13a	241.1 ± 4.3	0.0005 (***)	136.1 ± 6.2	0.0143 (*)	200.3 ± 17.7	0.0152 (*)	122.3 ± 6.0	0.0346 (*)
13b	200.5 ± 5.2	0.0014 (**)	124.5 ± 5.5	0.0240 (*)	176.4 ± 8.7	0.0064 (**)	116.3 ± 2.4	0.0110 (*)
13c	193.5 ± 8.5	0.0135 (*)	122.4 ± 13.7	0.1475 (ns)	173.8 ± 2.6	0.0078 (**)	118.0 ± 16.7	0.2682 (ns)
E2 (0.1 nM)	170.7 ± 20.9	0.0201 (*)	111.4 ± 21.6	0.5334 (ns)				

[a] Measured in duplicate, repeated twice (mean ± SD is presented) and normalized to vehicle-treated cells (100 %). Statistical analysis (*t*-test) was performed in GraphPad Prism5, (ns) non-significant, * $p < 0.05$, ** $p < 0.01$; *** $p < 0.001$.

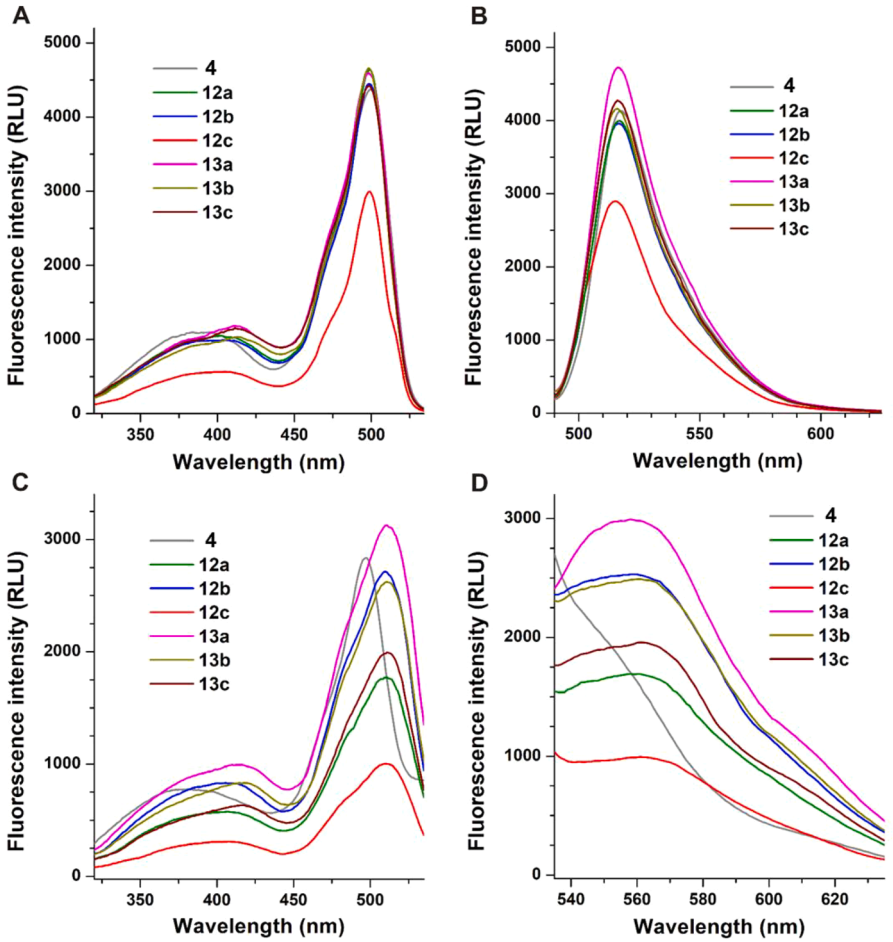

Fig. 5. Fluorescence excitation (A) and emission (B) spectra of 4 and E2 derivatives (each 10 μM) in DMF (λ_{ex} = 498 nm; λ_{em} = 515 nm; ex slit = 5 nm; em slit = 5 nm). Fluorescence excitation (C) and emission (D) spectra of 4 and E2 derivatives (each 10 μM) in sodium phosphate buffer (0.05 M, pH 7.4; λ_{ex} = 510 nm; λ_{em} = 560 nm; ex slit = 10 nm; em slit = 10 nm).

purified by flash chromatography with EtOAc/hexane, gradient from 1:9 to 3:7.

Compound **10a** was obtained as a white solid (391 mg, 96 %). M. p.:104.4–105.0 °C, R_f = 0.41[a]. Anal calcd. for $C_{22}H_{31}BrO_2$: C, 64.86; H, 7.67. Found: C, 64.94; H, 7.59. ^{1}H NMR ($CDCl_3$) δ (ppm): 0.78 (s, 3H, 18-H_3); 2.84 (m, 2H, 6-H_2); 3.48 (t, 2H, *J* = 6.6 Hz, Br-CH_2); 3.73 (t, 1H, *J* = 8.6 Hz, 17-H); 3.96 (t, 2H, *J* = 6.0 Hz, O—CH_2); 6.62 (d, 1H, *J* = 2.2 Hz, 4-H); 6.68 (dd, 1H, *J* = 8.6 Hz, *J* = 2.2 Hz, 2-H); 7.19 (d, 1H, *J* = 8.6 Hz, 1-H). ^{13}C NMR δ (ppm): 11.0 (C-18); 23.1; 26.3; 27.3; 27.9; 29.5; 29.8; 30.6; 33.5; 36.7; 38.8; 43.2 (C-13); 43.9; 50.0; 66.7 (O—CH_2); 81.9 (C-17); 111.9 (C-2); 114.4 (C-4); 126.3 (C-1); 132.7 (C-10); 138.0 (C-5); 156.7 (C-3).

Compound **10b** was obtained as a white solid (414 mg, 95 %). M.p.: 55.2–56.2 °C, R_f = 0.43[a]. Anal calcd. for $C_{24}H_{35}BrO_2$: C, 66.20; H, 8.10. Found: C, 66.39; H, 7.90. ^{1}H NMR ($CDCl_3$) δ (ppm): 0.78 (s, 3H, 18-H_3); 2.85 (m, 2H, 6-H_2); 3.42 (t, 2H, *J* = 6.8 Hz, Br-CH_2); 3.72 (t, 1H, *J* = 8.5 Hz, 17-H); 3.92 (t, 2H, *J* = 6.4 Hz, O—CH_2); 6.62 (d, 1H, *J* = 2.2 Hz, 4-H); 6.70 (dd, 1H, *J* = 8.6 Hz, *J* = 2.2 Hz, 2-H); 7.19 (d, 1H, *J* = 8.6 Hz, 1-H). ^{13}C NMR δ (ppm): 11.1 (C-18); 23.1; 25.3; 26.3; 27.3; 27.9; 29.2; 29.8; 30.6; 32.7; 33.9; 36.7; 38.9; 43.3 (C-13); 43.9; 50.0; 67.6 (O—CH_2); 81.9 (C-17); 112.0 (C-2); 114.5 (C-4); 126.3 (C-1); 132.5 (C-10); 137.9 (C-5); 156.9 (C-3).

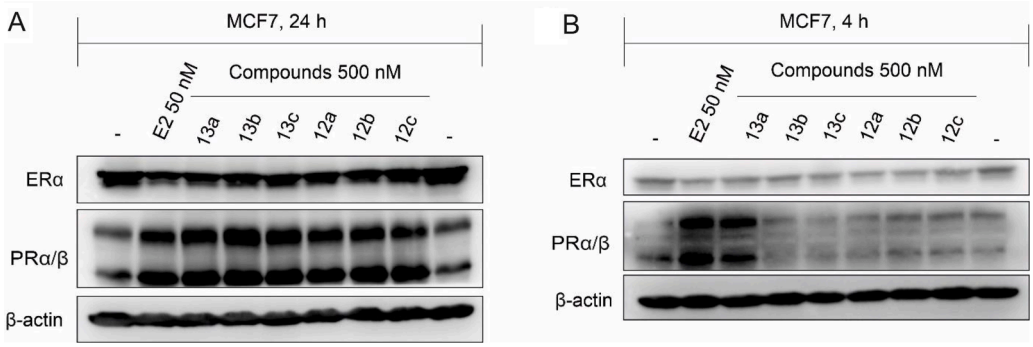

Fig. 6. Immunoblot analysis of crucial nuclear receptors in MCF7 treated for 24 h (A) or 4 h (B) with free E2 and 500 nM compounds in phenol red-free, CSS-supplemented medium. The level of β-actin served as a loading control. CSS, charcoal-stripped serum.

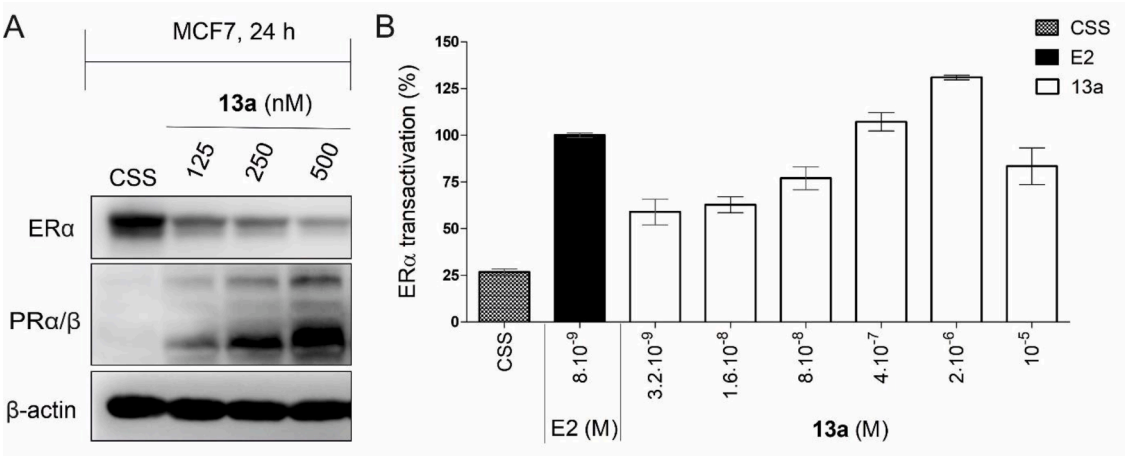

Fig. 7. (A) Immunoblot analysis of crucial nuclear receptors in MCF7 treated for 24 h with increased dose of **13a** in phenol red-free medium supplemented with CSS. The level of β-actin served as a loading control. (B) The effect of **13a** on the ER-mediated transcription in the dual luciferase reporter model. Transfected SKBR-3 cells were stimulated with 8 nM E2 (black column) or with different doses of **13a** for 24 h in phenol red-free CSS-medium and subsequently, the luciferases activities were measured in the cell lysate. Signal was normalized to the signal of 8 nM E2 (100 %). CSS, charcoal-stripped serum. .

Compound **10c** was obtained as a white solid (431 mg, 93 %). M.p.: 62.3–63.0 °C, $R_f = 0.50^a$. Anal calcd. for $C_{26}H_{39}BrO_2$: C, 67.38; H, 8.48. Found: C, 67.49; H, 8.35. ^{1}H NMR ($CDCl_3$) δ (ppm): 0.78 (s, 3H, 18-H_3); 2.85 (m, 2H, 6-H_2); 3.41 (t, 2H, J = 6.8 Hz, Br-CH_2); 3.73 (t, 1H, J = 8.5 Hz, 17-H); 3.92 (t, 2H, J = 6.5 Hz, O—CH_2); 6.63 (d, 1H, J = 2.2 Hz, 4-H); 6.70 (dd, 1H, J = 8.6 Hz, J = 2.2 Hz, 2-H); 7.19 (d, 1H, J = 8.6 Hz, 1-H). ^{13}C NMR δ (ppm): 11.0 (C-18); 23.1; 25.9; 26.3; 27.2; 28.1; 28.7; 29.2; 29.3; 29.8; 30.6; 32.8; 34.0; 36.7; 38.8; 43.2 (C-13); 43.9; 50.0; 67.8 (O—CH_2); 81.9 (C-17); 112.0 (C-2); 114.5 (C-4); 126.3 (C-1); 132.4 (C-10); 137.9 (C-5); 156.9 (C-3).

3.1.3. Synthesis of the steroidal azides *11a–c*

General procedure

A stirred solution of compound **10a, 10b** or **10c** (204, 218 or 232 mg, 0.5 mmol) in dry DMSO (5 mL) was treated with NaN_3 (33 mg, 0.5 mmol). The mixture was stirred for 2 h at rt, than poured into water (20 mL), and extracted with dichloromethane (3 × 10 mL). The combined organic layers were dried over sodium sulfate and the solvent was removed under reduced pressure. The residue was purified by flash chromatography with EtOAc/CH_2Cl_2 = 1/49 as an eluent.

Compound **11a** was obtained as a white solid (170 mg, 92 %). M.p.: 66.2–67.4 °C, $R_f = 0.47^b$. Anal calcd. for $C_{22}H_{31}N_3O_2$: C, 71.51; H, 8.46. Found: C, 71.64; H, 8.40. ^{1}H NMR ($CDCl_3$) δ (ppm): 0.78 (s, 3H, 18-H_3); 2.84 (m, 2H, 6-H_2); 3.35 (t, 2H, J = 6.8 Hz, N—CH_2); 3.73 (t, 1H, J = 8.6 Hz, 17-H); 3.96 (t, 2H, J = 5.7 Hz, O—CH_2); 6.62 (d, 1H, J = 2.2 Hz, 4-H); 6.68 (dd, 1H, J = 8.6 Hz, J = 2.2 Hz, 2-H); 7.19 (d, 1H, J = 8.6 Hz, 1-H). ^{13}C NMR δ (ppm): 11.0 (C-18); 23.1; 25.8; 26.3; 26.5; 27.2; 29.8; 30.6; 36.7; 38.8; 43.2 (C-13); 43.9; 50.0; 51.2; 67.0 (O—CH_2); 81.9 (C-17); 111.9 (C-2); 114.4 (C-4); 126.3 (C-1); 132.7 (C-10); 138.0 (C-5); 156.7 (C-3).

Compound **11b** was obtained as an oil (185 mg, 93 %). $R_f = 0.45^b$. Anal calcd. for $C_{24}H_{35}N_3O_2$:. C, 72.51; H, 8.87. Found: C, 72.63; H, 8.79. ^{1}H NMR ($CDCl_3$) δ (ppm): 0.78 (s, 3H, 18-H_3); 2.85 (m, 2H, 6-H_2); 3.27 (t, 2H, J = 6.89 Hz, N—CH_2); 3.73 (t, 1H, J = 8.55 Hz, 17-H); 3.93 (t, 2H, J = 6.37 Hz, O—CH_2); 6.63 (d, 1H, J = 2.2 Hz, 4-H); 6.70 (dd, 1H, J = 8.6 Hz, J = 2.2 Hz, 2-H); 7.19 (d, 1H, J = 8.6 Hz,1-H). ^{13}C NMR δ (ppm): 11.0 (C-18); 23.1; 25.7; 26.3; 26.5; 27.2; 28.8; 29.2; 29.8; 30.6; 36.7; 38.8; 43.2 (C-13); 43.9; 50.0; 51.4; 67.6 (O—CH_2); 81.9 (C-17); 111.9 (C-2); 114.4 (C-4); 126.3 (C-1); 132.5 (C-10); 137.9 (C-5); 156.8 (C-3).

Compound **11c** was obtained as a white solid (200 mg, 94 %). M.p.: 40.2–40.6 °C, $R_f = 0.46^b$. Anal calcd. for $C_{26}H_{39}N_3O_2$: C, 73.37; 9.24. Found: C, 73.49; H, 9.14. ^{1}H NMR ($CDCl_3$) δ (ppm): 0.78 (s, 3H, 18-H_3); 2.85 (m, 2H, 6-H_2); 3.25 (t, 2H, J = 7.0 Hz, N—CH_2); 3.73 (t, 1H, J = 8.5 Hz, 17-H); 3.92 (t, 2H, J = 6.5 Hz, O—CH_2); 6.62 (d, 1H, J = 2.2 Hz, 4-H); 6.70 (dd, 1H, J = 8.6 Hz, J = 2.2 Hz, 2-H); 7.19 (d, 1H, J = 8.6 Hz,1-H). ^{13}C NMR δ (ppm): 11.0 (C-18); 23.1; 25.9; 26.3; 26.6; 27.2; 28.8; 29.0; 29.2; 29.3; 29.8; 30.6; 36.7; 38.8; 43.3 (C-13); 43.9; 50.0; 51,4; 67.7 (O—CH_2); 81.9 (C-17); 111,9 (C-2); 114.4 (C-4); 126.3 (C-1); 132.4 (C-10); 137.9 (C-5); 156.9 (C-3).

3.1.4. Synthesis of triazolyl conjugates *12a–c*

General procedure

To a stirred solution of **11a, 11b** or **11c** (148, 159 or 170 mg, 0.40 mmol) in dry toluene (2 mL), Ph_3P (1.0 mg, 0.04 mmol), CuI (3.8 mg,

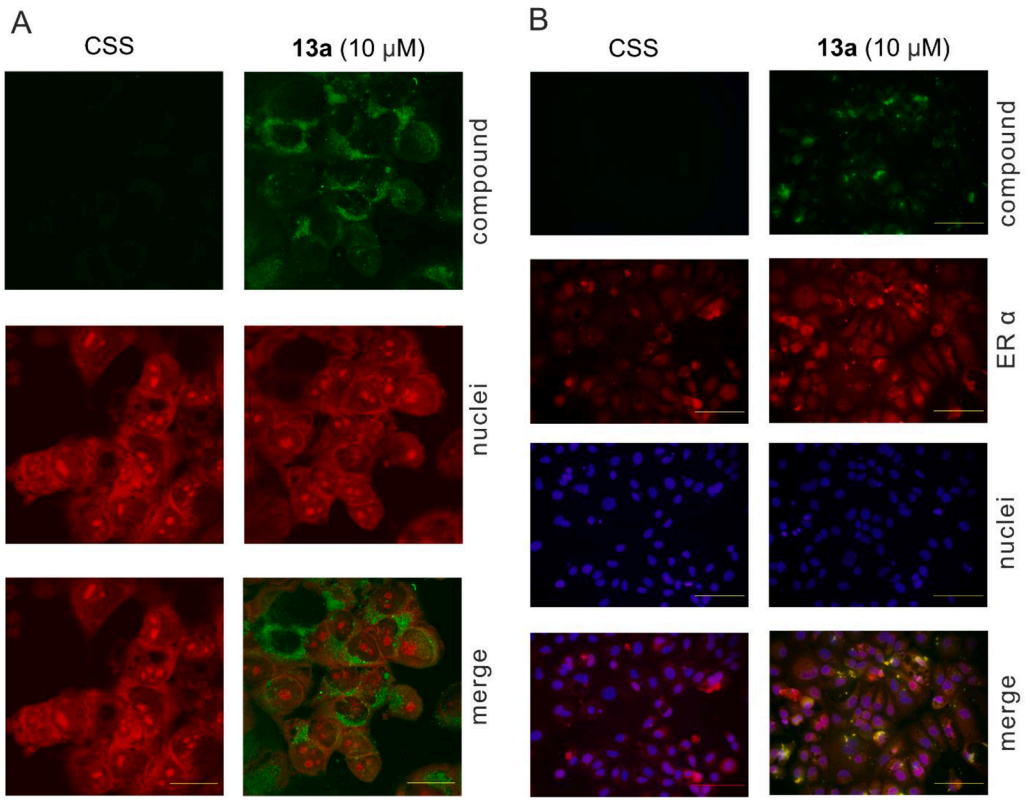

Fig. 8. **(A)** Confocal fluorescence microscopy pictures of MCF7 cultivated without or with 10 μM E2-BODIPY **13a** for 4 h in phenol red-free CSS medium and nuclei stained with propidium iodide. The scale bar represents 50 μm. **(B)** Fluorescence microscopy pictures of MCF7 cultivated with 10 μM **13a** for 4 h in phenol red-free CSS medium with nuclei stained with DAPI and ERα immuno-stained with Alexa Fluor 594 conjugated antibody. The scale bar represents 100 μm. CSS, charcoal-stripped serum.

0.02 mmol), DIPEA (0.21 mL, 1.2 mmol), and **4** (129 mg, 0.40 mmol) were added. The reaction mixture was kept at reflux temperature for 2 h and then allowed to cool down and evaporated in vacuo. The residue was purified by flash chromatography with EtOAc/CH_2Cl_2 = 1/9 as an eluent.

Compound **12a** was obtained as an orange solid (265 mg, 96 %). M. p.: 85.5–86.2 °C, R_f = 0.32[c] . Anal calcd. for $C_{40}H_{44}BF_2N_5O_3$: C, 69.46; H, 6.41. Found: C, 69.58; H, 6.29. ^{1}H NMR (DMSO-d_6) δ (ppm): 0.65 (s, 3H, 18-H_3); 2.75 (m, 2H, 6-H_2); 3.51 (m, 1H, 17-H); 3.91 (t, 2H, *J* = 6.2 Hz, N—CH_2); 4.45 (t, 2H, *J* = 6.8 Hz, O—CH_2); 4.49 (d, 1H, *J* = 4.76 Hz, 17-OH); 5.28 (s, 2H, BODIPY-O-CH_2); 6.58 (d, 1H, *J* = 2.2 Hz, 4-H); 6.64 (dd, 1H, *J* = 8.6 Hz, *J* = 2.2 Hz, 2-H); 6.69 (s, 2H, BODIPY-H); 7.05 (s, 2H); 7.14 (d, 1H, *J* = 8.6 Hz, 1-H); 7.28 (d, 2H, *J* = 8.6 Hz); 7.66 (d, 2H, *J* = 8.6 Hz); 8.10 (s, 2H); 8.32 (s, 1H, triazolyl C═CH). ^{13}C NMR δ (ppm): 11.2 (C-18); 22.7; 25.6; 25.9; 26.5; 26.8; 29.2; 29.8; 36.5; 38.5; 42.7 (C-13); 43.4; 49.1; 49.4; 61.4 (BODIPY-O-CH_2); 66.4 (O—CH_2); 79.9 (C-17); 111.8 (C-4); 113.9 (C-2); 114.9 (2C); 118.9 (2C); 124.6 (C═CH); 125.6 (2C); 126.0 (C-1); 131.3 (2C); 132.1 (C-10); 132.5 (2C); 133.9; 137.3 (C-5); 142.0; 143.9 (2C); 146.8; 156.1 (C-3); 160.6.

Compound **12b** was obtained as an orange solid (273 mg, 95 %). M. p.: 80.6–81.3 °C, R_f = 0.39[c]. Anal calcd. for $C_{42}H_{48}BF_2N_5O_3$: C, 70.09; H, 6.72. Found: 71.05; 6.59. ^{1}H NMR (DMSO-d_6) δ (ppm): 0.65 (s, 3H, 18-H_3); 2.75 (m, 2H, 6-H_2); 3.50 (m, 1H, 17-H); 3.86 (t, 2H, *J* = 6.3 Hz, N—CH_2); 4.39 (t, 2H, *J* = 6.9 Hz, O—CH_2); 4.48 (d, 1H, *J* = 4.8 Hz, 17-OH); 5.27 (s, 2H, BODIPY-O-CH_2); 6.57 (d, 1H, *J* = 2.2 Hz, 4-H); 6.63 (dd, 1H, *J* = 8.6 Hz, *J* = 2.2 Hz, 2-H); 6.69 (s, 2H, BODIPY-H); 7.04 (s, 2H, BODIPY-H); 7.13 (d, 1H, *J* = 8.6 Hz, 1-H); 7.27 (d, 2H, *J* = 8.6 Hz); 7.65 (d, 2H, *J* = 8.6 Hz); 8.10 (s, 2H); 8.30 (s, 1H, triazolyl C═CH). ^{13}C NMR δ (ppm): 11.2 (C-18); 22.7; 24.8; 25.5; 25.9; 26.8; 28.4; 29.2; 29.5; 29.8; 36.5; 38.5; 42.7 (C-13); 43.4; 49.3; 49.4; 61.4 (BODIPY-O-CH_2); 66.9 (O—CH_2); 79.9 (C-17); 111.8 (C-4); 113.9 (C-2); 114.9 (2C); 118.9 (2C); 124.6 (C═CH); 125.6 (2C); 126.0 (C-1); 131.5 (2C); 132.0 (C-10); 132.5 (2C); 133.9; 137.3 (C-5); 142.0; 143.9 (2C); 146.8; 156.3 (C-3); 160.6.

Compound **12c** was obtained as an orange solid (275 mg, 92 %). M. p.: 73.4–74.8 °C, R_f = 0.43[c]. Anal calcd. for $C_{44}H_{52}BF_2N_5O_3$: C, 70.68; H, 7.01. Found: C, 70.80; H, 6.90. ^{1}H NMR (DMSO-d_6) δ (ppm): 0.65 (s, 3H, 18-H_3); 2.74 (m, 2H, 6-H_2); 3.51 (m, 1H, 17-H); 3.86 (t, 2H, *J* = 6.4 Hz, N—CH_2); 4.38 (t, 2H, *J* = 6.9 Hz, O—CH_2); 4.49 (d, 1H, *J* = 4.2 Hz, 17-OH); 5.27 (s, 2H, BODIPY-O-CH_2); 6.57 (d, 1H, *J* = 2.2 Hz, 4-H); 6.63 (dd, 1H, *J* = 8.6 Hz, *J* = 2.2 Hz, 2-H); 6.69 (s, 2H); 7.05 (s, 2H); 7.13 (d, 1H, *J* = 8.6 Hz, 1-H); 7.27 (d, 2H, *J* = 8.6 Hz); 7.64 (d, 2H, *J* = 8.6 Hz); 8.10 (s, 2H, BODIPY H); 8.30 (s, 1H, triazolyl C═CH). ^{13}C NMR δ (ppm): 11.2 (C-18); 22.7; 25.3; 25.6; 25.9; 26.8; 28.2; 28.4; 28.6; 29.2; 29.6; 29.8; 36.5; 38.5; 42.7 (C-13); 43.4; 49.3; 49.4 (N—CH_2); 61.4 (BODIPY-O-CH_2); 67.0 (O—CH_2); 79.9 (C-17); 111.8 (C-4); 113.9 (C-2); 114.9 (2C); 118.9 (2C); 124.6 (C═CH); 125.6 (2C); 126.0 (C-1); 131.5 (2C); 131.9 (C-10); 132.6 (2C); 133.9; 137.3 (C-5); 142.0; 143.9 (2C); 146.8; 156.3 (C-3); 160.6.

*3.1.5. Synthesis of ether conjugates **13a–c***

71 mg (0.25 mmol) of **4a**, 138 mg (1.0 mmol) of anhydrous, pre-dried potassium carbonate, 5 mg (0.019 mmol) of 18-crown-6 was dissolved in 5 mL of dry toluene, then 204, 218 or 232 mg (0.50 mmol) of **10a, 10b** or **10c** was added to the solution. The reaction mixture was stirred at 110 °C for 24 h under N_2 atmosphere. It was worked up by adding 10 mL of water, 10 mL of ethyl acetate and stirred for about 10 min. The phases were intensively separated, and the aqueous phase was extracted with 10 mL of ethyl acetate. The combined organic phases were dried over sodium sulfate, and the solvent was removed under reduced pressure. The crude product was subjected to chromatographic separation with EtOAc/CH_2Cl_2 = 2/98 as an eluent.

Compound **13a** was obtained as an orange solid (139 mg, 91 %). M. p.: 83.6–84.0 °C, $R_f = 0.51$[a]. Anal calcd. for $C_{37}H_{41}BF_2N_2O_3$: C, 72.79; H, 6.77. Found: 72.85; H, 6.70. ^{1}H NMR (DMSO-d_6) δ (ppm): 0.66 (s, 3H, 18-H_3); 2.76 (m, 2H, 6-H_2); 3.51 (m, 1H, 17-H); 4.00 (t, 2H, J = 6.4 Hz, O—CH_2); 4.17 (t, 2H, J = 6.4 Hz, BODIPY-O-CH_2); 6.62 (d, 1H, J = 2.2 Hz, 4-H); 6.69 (overlapping multiplets, 3H); 7.06 (m, 2H); 7.15 (d, 1H, J = 8.7 Hz, 1-H); 7.17 (m, 2H); 7.63 (d, 2H, J = 8.7 Hz); 8.10 (s, 2H). ^{13}C NMR δ (ppm): 11.2 (C-18); 22.7; 25.2; 25.3; 25.9; 26.8; 29.1; 29.8; 36.5; 38.5; 42.7 (C-13); 43.5; 49.4; 66.8; 67.5; 79.9 (C-17); 111.9 (C-4); 114.0 (C-2); 114.7 (2C); 118.9 (2C); 125.2 (2C); 126.0 (C-1); 131.5 (2C); 132.0 (C-10); 132.6 (2C); 133.9; 137.3 (C-5); 143.8 (2C); 147.0; 156.3 (C-3); 161.4.

Compound **13b** was obtained as an orange solid (145 mg, 90 %). M. p.: 57.2–58.2 °C, $R_f = 0.53$[a]. Anal calcd. for $C_{39}H_{45}BF_2N_2O_3$: C, 73.35; H, 7.10. Found: C, 73.44; H, 7.01. ^{1}H NMR (DMSO-d_6) δ (ppm): 0.65 (s, 3H, 18-H_3); 2.74 (m, 2H, 6-H_2); 3.50 (m, 1H, 17-H); 3.92 (t, 2H, J = 6.43 Hz, O—CH_2); 4.11 (t, 2H, J = 6.4 Hz, BODIPY-O-CH_2); 6.59 (d, 1H, J = 2.2 Hz, 4-H); 6.65 (dd, 1H, J = 8.6 Hz, J = 2.2 Hz, 2-H); 6.69 (m, 2H); 7.06 (m, 2H); 7.14 (d, 1H, J = 8.6 Hz, 1-H); 7.16 (d, 2H, J = 8.6); 7.63 (m, 2H); 8.10 (s, 2H). ^{13}C NMR δ (ppm): 11.1(C-18); 22.7; 25.1 (2C); 25.2; 25.9; 26.8; 28.5; 28.6; 29.2; 29.8; 36.5; 38.5; 42.7 (C-13); 43.4; 49.4; 67.0; 67.7; 79.9 (C-17); 111.8 (C-4); 114.0 (C-2); 114.7 (2C); 118.9 (2C); 125.2 (2C); 126.0 (C-1); 131.5 (2C); 132.0 (C-10); 132.6 (2C); 133.9; 137.3 (C-5); 143.8 (2C); 146.9; 156.3 (C-3); 161.4.

Compound **13c** was obtained as an orange solid (153 mg, 92 %). M. p.: 48.1–51.0 °C, $R_f = 0.58$[a]. Anal calcd. for $C_{41}H_{49}BF_2N_2O_3$: C, 73.87; H, 7.41. Found: C, 73.95; H, 7.36. ^{1}H NMR (DMSO-d_6) δ (ppm): 0.65 (s, 3H, 18-H_3); 2.74 (m, 2H, 6-H_2); 3.50 (m, 1H, 17-H); 3.89 (t, 2H, J = 6.43 Hz, O—CH_2); 4.10 (t, 2H, J = 6.4 Hz, BODIPY-O-CH_2); 6.58 (d, 1H, J = 2.2 Hz, 4-H); 6.65 (dd, 1H, J = 8.6 Hz, J = 2.2 Hz, 2-H); 6.68 (m, 2H); 7.06 (m, 2H); 7.13 (d, 1H, J = 8.6 Hz, 1-H); 7.16 (d, 2H, J = 8.6 Hz); 7.62 (m, 2H); 8.10 (s, 2H). ^{13}C NMR δ (ppm): 11.2 (C-18); 22.7; 25.2; 25.3; 25.9; 26.8; 28.4; 25.5 (2C); 28.6; 29.1; 29.8; 36.5; 38.5; 42.7 (C-13); 43.5; 49.4; 67.1; 67.8; 79.9 (C-17); 111.9 (C-4); 114.0 (C-2); 114.7 (2C); 118.9 (2C); 125.2 (2C); 126.0 (C-1); 131.3 (2C); 132.0 (C-10); 132.6 (2C); 133.9; 137.3 (C-5); 143.8 (2C); 147.0; 156.3 (C-3); 161.4.

3.2. In silico investigations

Preparation of ligands. All ligands were built in Maestro (Schrödinger 2021). Raw structures were minimized using MOPAC, semiempirical quantum chemistry program package with PM7 parametrization (MOPAC 2016). The gradient norm was set to 0.001. Force calculations with positive force constant matrices were applied on the energy-minimized structures. These energy-minimized structures were used for docking calculations.

Preparation of target. The human estrogen receptor alpha ligand binding domain (hERα LBD) was used as target in this study. The apo structure was obtained from the Protein Data Bank (Berman et al., 2000) (PDB code: 2b23; (Nettles et al., 2008)). Water molecules, ions, and coactivator peptide fragment were cut from the original experimental structure. The holo target structure based on PDB code 3q95 was reused from our previous study (Bálint et al., 2017).

Docking calculations. Focused docking calculations were performed with Autodock 4.2.6 (Berman et al., 2000) using the minimized and equilibrated ligand structures on target's region including the classical and alternative binding site (CBS, ABS) determined in previous study (Bálint et al., 2017). Grid box was generated by Autogrid 4.2.6. (Morris et al., 2009) with 102 gridpoints along all axes spacing of 0.375 Å, centered to cover CBS, ABS, and bulk to have even the longest ligand enough place to find the best docking pose. AutodockTools (Morris et al., 2009) was used to assign Gasteiger–Marsili partial charges to both the ligand and the receptor atoms beside a united-atom representation for non-polar moieties. The receptor was treated rigidly; however, flexibility was allowed at all active torsions of the ligands. Lamarckian genetic algorithm was used for global search. 10 docking runs were performed for all ligands. Ligand conformations were ranked by the corresponding calculated interaction energy values and subsequently clustered using a tolerance of 3.5 Å root mean square deviation (RMSD) between cluster members. The rank 1 was analyzed and selected as representative structure for each ligand except compound **13a**, where the rank 2 was selected. Parameters of carbon atom were applied for boron in docking calculations for all ligands.

3.3. Cell lines

The MCF7 cell line (purchased from ECACC) and the SKBR-3 (purchased from ATCC) were both grown in phenol red-free DMEM-medium. To avoid activation of ER by steroids present in fetal bovine serum (FBS), media were supplemented by charcoal-stripped fetal bovine serum (CSS), which is a steroid-depleted serum. The media contained 4 mM glutamine, 100 IU/ml penicillin and 100 μg/ml streptomycin as well. Cells were cultivated in a humidified incubator in 5 % CO_2 atmosphere at 37 °C.

3.4. Proliferation assay

Both cell lines were seeded into the 96-well tissue culture plates in density of 5000 cells/well. The other day, solutions of compounds along with the E2 were added in different concentrations for 72 h. Then, the resazurin (Sigma Aldrich) solution was added for 4 h. The fluorescence of resorufin was subsequently measured at 544 nm/590 nm (excitation/emission) using a Fluoroskan Ascent microplate reader (Labsystems). Percentual viability was calculated and normalized to the signal of control treated by vehicle. The dose response curves were evaluated using GraphPad Prism 5.

3.5. Western blot

The cells were cultivated and treated as usual (details of the treatment are specified in results obtained from separate experiments). Upon treatments, cells were pelleted by centrifugation at 1.000 *g*, washed with PBS and kept frozen at - 80 °C. Samples were thawed and lysed based on the standard protocol in RIPA lysis buffer, sonicated and centrifuged at 14.000 *g* for 30 min. Concentrations of proteins were measured and balanced within samples. Proteins were denatured in SDS-loading buffer, undergone the SDS-PAGE and they were transferred onto nitrocellulose membranes. Membranes were blocked in BSA solution, incubated with primary antibodies, washed and incubated with peroxidase-conjugated secondary antibodies. Peroxidase activity was detected by SuperSignal West Pico reagents (Thermo Scientific) and visualized using a CCD camera LAS-4000 (Fujifilm). Primary antibodies purchased from Santa Cruz Biotechnology (anti-β-actin, clone C4). Specific antibodies purchased from Cell Signaling Technology (anti-ERα, clone D6R2W; anti-PRα/β, clone D8Q2J; anti-rabbit secondary antibody (porcine anti-rabbit immunoglobulin serum); anti-mouse secondary antibody (rabbit anti-mouse IgG, clone D3V2A). Antibodies were diluted in 4 % BSA and 0.1 % Tween 20 in TBS.

3.6. Dual luciferase reporter gene assay

The dual-luciferase assay based on a bicistronic luciferase vector coding RLUC (renilla luciferase) showing constitutive expression, and FLUC (firefly luciferase) inducible in response to ER activation was performed as previously published (Vonka et al., 2023). Briefly, SKBR-3 cells underwent nucleofection according to the manufacturer's instructions using Amaxa Cell Line Nucleofector (Lonza Cologne AG). For transfection of 1×10^6 cells, 2 μg of vector DNA were used (the ratio of pcDNA3_hERα and pcDNA3_FLUC_RLUC was 1:2). Transfected cells were seeded into 96-well plates in density 30 000 cells/well and, after 24 h, analyzed compounds were applied at various concentration along with estradiol in phenol red-free CSS-medium. Upon treatment,

cultivation medium was discarded, cells were washed with PBS and lysed in 1x Passive lysis buffer (Promega Corporation). Further, firefly bioluminescence was measured (Tecan M200-Pro, Biotek) using filter GREEN1 (560 nm). Reaction was stopped by 300 mM EDTA and bioluminescence of renilla luciferase was determined using filter BLUE1 (480 nm). The ratio of both signals (FLUC/RLUC) in cells was normalized to the ratio of cells treated with 8 nM E2 (100 %).

3.7. Fluorescence intensity measurements and quantification

Cells were seeded into the FluoroNunc™ 96-well plate with clear bottom in density of 20.000 cells/well in phenol-red free CSS supplemented media. The next day, cells were treated with our derivatives for 4 h. Next, cells were washed with PBS twice, then 100 μl of the PBS was added to the wells and fluorescence of internalized E2-BODIPY derivatives was measured. Wells were measured with multiple reads (25 reads/well) by fluorescence top read with excitation and emission wavelengths 515 nm and 560 nm, respectively. Three biological replicates were made, from which the mean from multiple reads was used to calculate the mean and SD from replicates. Values of fluorescence intensity were normalized to the sample with highest value (to be 100 %).

3.8. Fluorescent microscopy

Cells were cultivated and stained using novel derivatives or Hoechst 33,342 or propidium iodide in 8-well chamber μ-Slide (IBIDI). After the treatment, cells were observed under a fluorescence microscope (Olympus IX51, Japan). For fluorescence microscopy of nuclei, after the treatment, cells were permeabilized by 2 M HCl with 0.5 % Triton X-100 for 15 min. The sample was pelleted by centrifugation at 1000 *g* for 10 min. The cytosolic supernatant was discarded and nuclei were neutralized using 0.1 M $Na_2B_4O_7$. Nuclei were washed in filtered PBS, transferred into microscopic slide and observed under a fluorescence microscope.

For imuno-staining, we cultivated and treated the cells with the compounds in μ-Slide 8 (IBIDI) the same way. After treatment the cells were washed with PBS and fixed by an addition of ice-cold methanol: acetone (1:1) for 10 min. The fixation solution was discarded and the slide was kept to dry for an extra 10 min and stored in −20 °C. Then, the cells were re-hydrated with PBS-T (PBS with 1 % Tween). Cells were blocked in the solution of 1 % bovine serum albumin (BSA) in PBS-T for 1 h, then they were incubated with primary antibody against ERα (clone D8H8, Santa Cruz Biotechnology) overnight. After incubation, cells were washed with PBS-T three times followed by incubation with secondary antibody (goat anti-mouse with Alexa Fluor 594, clone A-11,032, ThermoFisher) for 1 h. Next, cells were washed with PBS-T twice and with PBS once, then staining with DAPI (Merck) was performed for 10 min, cells were washed with PBS twice, covered with Mowiol (Merck) and observed using fluorescence microscope (Olympus IX51, Japan).

Confocal Leica TCS SP5 X (Leica Microsystems Heidelberg, Germany) was used for confocal microcopy imaging. Cells were again cultivated and treated with the compounds in μ-Slide 8 (IBIDI) the same way, after treatment the cells were washed with PBS and fixed by an addition of ice-cold methanol:acetone (1:1) for 10 min. The fixation solution was discarded and slide was left to dry for an extra 10 min. Upon rehydration, nuclei staining with propidium iodide was performed for 30 min, cells were washed with PBS and covered with Mowiol and visualised. Image analysis was performed in ImageJ, as well as channel merge. The quatification and analysis of co-localisation of green E2-BODIPY signal of **13a** with nuclei or ERα signal was also performed using ImageJ. Co-localisation parameters were calculated using the JACoP plugin from at least two representative replicate pictures. The Manders' coefficients were then used to evaluate the co-localisation of signals by percentage of overlap.

3.9. Detection of *13a* in cell's nuclei

Cells were treated with test compounds, they were harvested by trypsinisation, washed with PBS and fixed with 70 % ethanol. After rehydration, cells were permeabilised by 2 M HCl, 0.5 % Triton X-100. Following neutralization and wash with PBS, the nuclei were isolated and stained with propidium iodide (ThermoFisher, USA) at concentration of 10 μg/ml, for 30 min. Nuclei were analyzed by flow cytometry with a 488 nm laser (BD FACS Verse with BD FACSuite software, version 1.0.6.). The whole population of the analysed nuclei was counted using the side and forward scatter. The percent of **13a-**positive nuclei was calculated as a ratio of green-fluorescent events and all events within every sample. The statistical difference between cells treated by vehicle and several doses of compound was calculated using *t*-test in GraphPad Prism5.

3.10. Estrogen receptor competitive binding assay

The ERα competitive binding assay with the radioligand [3*H*]estradiol was performed by Eurofins Discovery according to their manufactured protocol. The assay ran at 22 °C for 2 h and the compound was tested at seven concentrations for Ki determination in duplicate. Diethylstilbestrol served as an assay control.

3.11. Data processing and statistics

Data from biological replicates were processes as usual, mean and SD were calculated and the graphs were constructed in GraphPad Prism 5 (GraphPad Software, San Diego, USA). Statistical differences between controls and treatments were assessed by unpaired *t*-test with a two-tailed p-value at confidence interval 95 %. A p-value higher than 0.05 was considered as non-significant (ns) and the significance was annotated as follows: * $p < 0.05$, ** $p < 0.01$; *** $p < 0.001$.

4. Conclusions

In conclusion, we have developed efficient fluorescent labeling strategies for the most potent estrogen E2. Our methodology was based on labeling at the 3-OH function, which is one of the main oxygen functionalities in estrogens. Steroidal and fluorescent (BODIPY) building blocks were connected indirectly by the introduction of freely rotating alkyl linkers differing in the number of carbon atoms. Conjugations were performed *via* Cu(I)-catalyzed azide–alkyne click or etherification reactions. Interactions of the conjugates with ER were investigated using molecular docking calculations in comparison with estradiol. The conjugates occupy the canonical binding site of estradiol on hERα with a slightly lower affinity then E2 and DES. All compounds displayed reasonable estrogenic activity, stimulated the ER transcriptional activity and downstream signaling. The most potent compound **13a** induced the transcriptional activity of ER in dose-dependent manner in reporter model. The green fluorescent signal was localized mainly in the cytosol, but it was found in nucleus in the dose-dependent manner as well. The fluorescent signal of candidate compound **13a** did not clearly co-localized with nuclear signal, but clearly co-localized with signal of ERα. The newly synthesized estradiol-BODIPY conjugates might serve as a starting point to develop good candidates for the investigation of estrogen uptake, transport, biotransformation and protein binding properties (Felion et al., 2022; Gai and Sun, 2022). Monitoring these processes is of high importance not only regarding the estrogenic action, but in other biological relationships, including neuroprotective behavior. Additionally, because of the "visibility" of fluorescent estrogens, new important biological actions might also be identified.

CRediT authorship contribution statement

Miroslav Peřina: Writing – review & editing, Writing – original

draft, Methodology, Investigation, Data curation, Conceptualization. **Rita Börzsei:** Writing – original draft, Visualization, Software, Methodology, Data curation, Conceptualization. **Henrietta Ágoston:** Writing – original draft, Investigation, Conceptualization. **Tamás Hlogyik:** Investigation. **Miklós Poór:** Writing – review & editing, Writing – original draft, Investigation. **Réka Rigó:** Investigation. **Csilla Özvegy-Laczka:** Supervision. **Gyula Batta:** Methodology, Conceptualization. **Csaba Hetényi:** Writing – review & editing, Writing – original draft, Supervision, Methodology, Conceptualization. **Veronika Vojáčková:** Investigation. **Radek Jorda:** Writing – review & editing, Writing – original draft, Supervision, Methodology, Investigation, Conceptualization. **Erzsébet Mernyák:** Writing – review & editing, Writing – original draft, Supervision, Methodology, Funding acquisition, Conceptualization.

Data availability

Data will be made available on request.

Acknowledgments

This work was supported by National Research, Development and Innovation Office-NKFIH through projects OTKA SNN 124329 and OTKA SNN 139323. The work was supported by the PTE ÁOK-KA 2021/KA-2021–39. The project has been supported by the European Union, co-financed by the European Social Fund, project name and code: Comprehensive Development for Implementing Smart Specialization Strategies at the University of Pécs, EFOP-3.6.1–16–2016–00004. We acknowledge the support from the Governmental Information Technology Development Agency, Hungary. We acknowledge that the results of this research have been achieved using the DECI resource Archer2 based in the UK at the National Supercomputing Service with support from the PRACE aisbl. Project no. TKP2021-EGA-16 has been implemented with the support provided from the National Research, Development and Innovation Fund of Hungary, financed under the EGA 16 funding scheme. Project no. TKP2021-EGA-13 has been implemented with the support provided from the National Research, Development and Innovation Fund of Hungary, financed under the EGA-13 funding scheme. Project no. RRF-2.3.1–21–2022–00015 has been implemented with the support provided by the European Union. The work was also supported by the Palacký University Olomouc (IGA_PRF_2023_012). The authors thank Vivien Szabó for the synthesis of certain starting materials.

Supplementary materials

Supplementary material associated with this article can be found, in the online version, at doi:10.1016/j.ejps.2024.106813.

References

Miller, W.L., Auchus, R.J., 2011. The molecular biology, biochemistry, and physiology of human steroidogenesis and its disorders. Endocr. Rev. 32, 81–151. https://doi.org/10.1210/er.2010-0013.

Gupta, A., Kumar, S.B., Negi, A.S., 2013. Current status on development of steroids as anticancer agents. J. Steroid Biochem. Mol. Biol. 137, 242–270. https://doi.org/10.1016/j.jsbmb.2013.05.011.

Hong, Y., Chen, S., 2011. Aromatase, estrone sulfatase, and 17β-hydroxysteroid dehydrogenase: structure-function studies and inhibitor development. Mol. Cell. Endocrinol. 340, 120–126. https://doi.org/10.1016/j.mce.2010.09.012.

Marchais-Oberwinkler, S., Henn, C., Möller, G., Klein, T., Negri, M., Oster, A., Spadaro, A., Werth, R., Wetzel, M., Xu, K., Frotscher, M., Hartmann, R.W., Adamski, J., 2011. 17β-Hydroxysteroid dehydrogenases (17β-HSDs) as therapeutic targets: protein structures, functions, and recent progress in inhibitor development. J. Steroid Biochem. Mol. Biol. 125, 66–82. https://doi.org/10.1016/j.jsbmb.2010.12.013.

Azcoitia, I., Arevalo, M.A., De Nicola, A.F., Garcia-Segura, L.M., 2011. Neuroprotective actions of estradiol revisited. Trends Endocrinol. Metabol. 22, 467–473.

Pelletier, G., 2010. Steroidogenic enzymes in the brain: morphological aspects. Prog. Brain Res. 181, 193–207. https://doi.org/10.1016/S0079-6123(08)81011-4.

Cespedes Rubio, A.E., Perez-Alvarez, M.J., Lapuente Chala, C., Wandosell, F, 2018. Sex steroid hormones as neuroprotective elements in ischemia models. J. Endocrinol. 237, R65–R81. https://doi.org/10.1530/JOE-18-0129.

Ulrich, G., Ziessel, R., Harriman, A., 2008. The chemistry of fluorescent BODIPY dyes: versatility unsurpassed. Angew. Chem. Int. Ed. 47, 1184–1201. https://doi.org/10.1002/anie.200702070.

Loudet, A., Burgess, K., 2007. BODIPY dyes and their derivatives: syntheses and spectroscopic properties. Chem. Rev. 107, 4891–4932. https://doi.org/10.1021/cr078381n.

Karolin, J., Johansson, L.B-A., Strandberg, L., Ny, T., 1994. Fluorescence and absorption spectroscopic properties of dipyrromethemeboron difluoride (BODIPY) derivatives in liquids, lipid membranes, and proteins. J. Am. Chem. Soc. 116, 7801–7806. https://doi.org/10.1021/ja00096a042.

Haugland, R.P., 1996. Handbook of fluorescent probes and research chemicals. In: Spence, Michelle T., Johnson, Iain D. (Eds.), Molecular Probes, 6th edEd. Eugene.

Osati, S., Ali, H., van Lier, J.E., 2016. BODIPY-steroid conjugates: syntheses and biological applications. J. Porphyrins Phthalocyanines 20, 1–15. https://doi.org/10.1142/S1088424616300019.

Osati, S., Ali, H., Guerin, B., van Lier, J.E., 2017. Synthesis and spectral properties of estrogen- and androgen-BODIPY conjugates. Steroids. 123, 27–36. https://doi.org/10.1016/j.steroids.2017.04.007.

Liang, L., Astruc, D., 2011. The Copper(I)-catalyzed alkyne-azide cycloaddition (CuAAC) "click" reaction and its applications. an overview coord. Chem. Rev. 255, 2933–2945. https://doi.org/10.1016/j.ccr.2011.06.028.

Langhals, H., Obermeier, A., 2008. A Click Reaction for Fluorescent Labelling: application of the 1,3-Dipolar cycloaddition reaction. Eur. J. Org. Chem. 36, 6144–6151. https://doi.org/10.1002/ejoc.200800805.

Felion, C., Lopez-Gonzalez, R., Sewell, A.L., Marquez, R., Gauchotte-Lindsay, C., 2022. BODIPY-labeled estrogens for fluorescence analysis of environmental microbial degradation. ACS. Omega 7 (45), 41284–41295. https://doi.org/10.1021/acsomega.2c05002.

Bacsa, I., Konc, C., Orosz, A.B., Kecskeméti, G., Rigó, R., Özvegy-Laczka, C., Mernyák, E., 2018. Synthesis of novel C-2- or C-15-labeled BODIPY-estrone conjugates. Molecules. 23, 821–834. https://doi.org/10.3390/molecules23040821.

Jirikowski, G.F.; Reimar, K. Steroid-Styrylfarbstoff-Konjugate Zur Simulation und Direkten Lichtoptischen Detektion des Verhaltens von Steroiden im Lebenden Biologischen Gewebe und in Gegenwart von Steroidbindenden Proteinen. DE 102010027016A1.

Szabo, J., Bacsa, I., Wölfling, J., Schneider, G., Zupko, I., Varga, M., Herman, B.E., Kalmar, L., Szecsi, M., Mernyak, E., 2016. Synthesis and in vitro pharmacological evaluation of N-[(1-benzyl-1,2,3-triazol-4-yl)methyl]-carboxamides on D-secoestrone scaffolds. J. Enzyme Inhib. Med. Chem. 31, 574–579. https://doi.org/10.3109/14756366.2015.1050008. /.

Kadar, Z., Kovacs, D., Frank, E., Schneider, G., Huber, J., Zupko, I., Bartok, T., Wölfling, J., 2011. Synthesis and In Vitro Antiproliferative Activity of Novel Androst-5-ene Triazolyl and Tetrazolyl Derivatives. Molecules. 16, 4786–4806. https://doi.org/10.3390/molecules16064786.

Kadar, Z., Molnar, J., Schneider, G., Zupko, I., Frank, E., 2012. A facile 'click' approach to novel 15β-triazolyl-5α-androstane derivatives, and an evaluation of their antiproliferative activities in vitro. Bioorg. Med. Chem. 20, 1396–1402. https://doi.org/10.1016/j.bmc.2012.01.008.

Mernyak, E., Kovacs, I., Minorics, R., Sere, P., Czegany, D., Sinka, I., Wölfling, J., Schneider, G., Ujfaludi, Z., Boros, I., Ocsovszki, I., Varga, M., Zupkó, I., 2015. Synthesis of trans-16-triazolyl-13α-methyl-17-estradiol diastereomers and the effects of structural modifications on their in vitro antiproliferative activities. J. Steroid Biochem. Mol. Biol. 150, 123–134. https://doi.org/10.1016/j.jsbmb.2015.04.001.

Szabó, J., Pataki, Z., Wölfling, J., Schneider, G., Bózsity, N., Minorics, R., Zupkó, I., Mernyák, E., 2016. Synthesis and biological evaluation of 13α-estrone derivatives as potential antiproliferative agents. Steroids. 113, 14–21. https://doi.org/10.1016/j.steroids.2016.05.010.

Pedersen, D.S., Abell, A., 2011. 1,2,3-Triazoles in peptidomimetic chemistry. Eur. J. Org. Chem. 13, 2399–2411. https://doi.org/10.1002/ejoc.201100157.

Bálint, M., Jeszenői, N., Horváth, I., van der Spoel, D., Hetényi, C., 2017. Systematic exploration of multiple drug binding sites. J. Cheminform. 9 https://doi.org/10.1186/s13321-017-0255-6.

Norman, A.W., Mizwicki, M.T., Norman, D.P.G., 2004. Steroid-hormone rapid actions, membrane receptors and a conformational ensemble model. Nat. Rev. Drug Discov. 3, 27–41. https://doi.org/10.1038/nrd1283.

van Hoorn, W.P, 2002. Identification of a second binding site in the estrogen receptor. J. Med. Chem. 45, 584–589. https://doi.org/10.1021/jm0109661.

Kousteni, S., Chen, J.R., Bellido, T., Han, L., Ali, A.A., O'Brien, C.A., Plotkin, L., Fu, Q., Mancino, A.T., Wen, Y., Vertino, A.M., Powers, C.C., Stewart, S.A., Ebert, R., Parfitt, A.M., Weinstein, R.S., Jilka, R.L., Manolagas, S.C., 2002. Reversal of bone loss in mice by nongenotropic signaling of sex steroids. Science 298, 843–846. https://doi.org/10.1126/science.1074935.

Anstead, G.M., Carlson, K.E., Katzenellenbogen, J.A., 1997. The estradiol pharmacophore: ligand structure-estrogen receptor binding affinity relationships and a model for the receptor binding site. Steroids. 62, 268–303. https://doi.org/10.1016/s0039-128x(96)00242-5.

Brzozowski, A.M., Pike, A.C., Dauter, Z., Hubbard, R.E., Bonn, T., Engström, O., Ohman, L., Greene, G.L., Gustafsson, J.A., Carlquist, M., 1997. Molecular basis of agonism and antagonism in the oestrogen receptor. Nature 389, 753–758. https://doi.org/10.1038/39645.

Marino, M., Galluzzo, P., Ascenzi, P., 2006. Estrogen signaling multiple pathways to impact gene transcription. Curr. Genomics 7, 497–508.

Fazzari, A., et al., 2001. The control of progesterone receptor expression in MCF-7 breast cancer cells: effects of estradiol and sex hormone binding globulin (SHBG). Mol. Cell. Endocrinol. 172, 31–36.

Farfan-Paredes, M., Gonzalez-Antonio, O., Tahuilan-Anguiano, D.E., Peon, J., Ariza, A., Lacroix, P.G., Santillan, R., Farfan, N., 2020. Physicochemical and computational insight of ^{19}F NMR and emission properties of meso-(o-aryl)-BODIPYs. New. J. Chem. 44, 19459–19471. https://doi.org/10.1039/d0nj02576c.

Schrödinger, 2021. Release 2023-1: Maestro. Schrödinger, LLC, New York, NY.

MOPAC 2016, James J. P. Stewart, stewart computational chemistry, Colorado Springs, CO, USA, HTTP://OpenMOPAC.net (2016).

Berman, H.M., Westbrook, J., Feng, Z., Gilliland, G., Bhat, T.N., Weissig, H., Shindyalov, I.N., Bourne, P.E., 2000. The protein data bank. Nucleic Acids Res. 28, 235–242. https://doi.org/10.1093/nar/28.1.235.

Nettles, K.W., Bruning, J.B., Gil, G., Nowak, J., Sharma, S.K., Hahm, J.B., Kulp, K., Hochberg, R.B., Zhou, H., Katzenellenbogen, J.A., Katzenellenbogen, B.S., Kim, Y., Joachmiak, A., Greene, G.L., 2008. NFκB selectivity of estrogen receptor ligands revealed by comparative crystallographic analyses. Nat. Chem. Biol. 4, 241–247. https://doi.org/10.1038/nchembio.76.

Morris, G.M., Huey, R., Lindstrom, W., Sanner, M.F., Belew, R.K., Goodsell, D.S., Olson, A.J., 2009. AutoDock4 and AutoDockTools4: automated docking with selective receptor flexibility. J. Comput. Chem. 30, 2785–2791. https://doi.org/10.1002/jcc.21256.

Vonka, P., Rarova, L., Bazgier, V., Tichy, V., Kolarova, T., Holcakova, J., Berka, K., Kvasnica, M., Oklestkova, J., Kudova, E., Strnad, M., Hrstka, R., 2023. Small change - big consequence: the impact of C15-C16 double bond in a D-ring of estrone on estrogen receptor activity. J. Steroid. Biochem. Mol. Biol., 106365 https://doi.org/10.1016/j.jsbmb.2023.106365.

Gai, L., Sun, W., 2022. Recent advances in estrogen receptor-targeted probes conjugated to BODIPY dyes. Steroids. 183, 109031 https://doi.org/10.1016/j.steroids.2022.109031.